Supporting Information

Conversion of Methanol to Hydrocarbons over H-MCM-22 Zeolite: Deactivation Behaviours related to Acid Density and Distribution

Tingyu Liang[a], Jialing Chen[b,*], Sen Wang[c], Pengfei Wang[c], Zhangfeng Qin[c], Fang Jin[a], Mei Dong[c], Jianguo Wang[c], Weibin Fan[c]

[a] *Key Laboratory for Green Chemical Process of Ministry of Education, and Hubei Key Laboratory of Novel Reactor & Green Chemical Technology, School of Chemical Engineering & Pharmacy, Wuhan Institute of Technology, Wuhan 430205, China*

[b] *Key Laboratory of Hubei Province for Coal Conversion and New Carbon Materials, School of Chemistry and Chemical Engineering, Wuhan University of Science and Technology, Wuhan 430081, China*

[c] *State Key Laboratory of Coal Conversion, Institute of Coal Chemistry, Chinese Academy of Sciences, P.O. Box 165, Taiyuan, Shanxi 030001, PR China*

* Corresponding authors: Tel.: +86 027 68862335. E-mail addresses: chenjialing@wust.edu.cn.

As the **Supporting Information** of the manuscript "*Conversion of Methanol to Hydrocarbons over H-MCM-22 Zeolite: Deactivation Behaviours related to Acid Density and Distribution*", following materials are provided:

(1) The Brϕnsted and Lewis acid density with different strength in the H-M22-*x* zeolites (Table S1);

(2) Catalytic performance of the H-M22-*x* zeolites in MTH (Table S2);

(3) The linear relationship between aluminum concentration from ICP-AES determination and total acid density from quantitative results of NH_3-TPD profiles in H-M22-*x* zeolites (Figure S1);

(4) Determination of acid distribution and acid strength for H-M22-x zeolites by FT-IR spectra of pyridine adsorption（Py-IR） and 2,6-di-tert-butylpyridine adsorption（DTBPy-IR）. (Figure S2);

(5) Deconvolution of the ^{27}Al and ^{29}Si MAS NMR spectra of the H-M22-*x* zeolites (Figure S3–S5);

(6) P/E ratio and C_4-HTI as a function of time on stream in MTH over H-M22-*x* zeolites (Figure S6);

(7) GC-MS total ion chromatograms of carbonaceous species retained in H-M22-x zeolites at the time on stream (TOS) of 3 h and 15 h for MTH at 450 ^{o}C with a methanol WHSV of 2 h^{-1} over H-M22-x zeolites (Figure S7);

(8) UV-vis spectra of completely deactivated H-M22-x zeolites (Figure S8).

Table S1. The Brϕnsted and Lewis Acid Density with Different Strength in the H-M22-*x* Zeolites.

Zeolite	B_{ext} [a] (μmol g^{-1})	BAS density [b] (μmol g^{-1})			LAS density [b] (μmol g^{-1})		
		weak	medium	strong	weak	medium	strong
H-M22-15	62	24	42	379	99	27	116
H-M22-30	45	25	36	203	82	6	68
H-M22-50	25	27	34	130	10	11	14
H-M22-70	24	26	36	100	12	4	9
H-M22-90	12	26	34	59	10	0	0

[a] The amount of external Brϕnsted acid sites was calculated from the DTBPy-IR spectra.

[b] The amount of BAS and LAS with different acid strength was estimated from the quantities of Brϕnsted acid sites (BAS) and Lewis acid sites (LAS) determined by Py-IR at different temperatures; the differences in BAS (or LAS) between 150 and 250 °C, between 250 and 350 °C, and remained BAS (or LAS) at 350 °C correspond to weak, medium, and strong acid sites, respectively.

Table S2. Catalytic Performance of the H-MCM-22 Zeolites with Different Si/Al Ratios in MTH. [a]

Zeolite	Methanol conversion [b] (%)	Product distribution [b] (%)							P/E [c]	C_4–HTI [d]	Lifetime [e] (h)
		C_{1-5}^0	$C_2^=$	$C_3^=$	$C_4^=$	$C_5^=$	aromatics	others			
H-M22-15	99.9	21.6	9.8	26.9	12.1	3.6	20.7	5.3	2.7	0.33	36
H-M22-30	99.8	9.5	5.1	42.4	18.5	10.7	8.5	5.3	8.3	0.12	60
H-M22-50	99.8	5.7	3.5	47.4	19.8	14.2	3.9	5.5	13.5	0.07	49
H-M22-70	99.8	4.4	3.2	48.2	20.3	16.4	2.4	5.1	15.1	0.05	39
H-M22-90	99.3	5.1	2.9	45.6	20.1	17.3	1.4	7.6	15.7	0.04	14

[a] The MTH reaction was carried out at 450 °C at atmosphere pressure with a methanol WHSV of 2 h^{-1}; the feed was diluted by 66.7 vol.% nitrogen.

[b] The methanol conversion and product distribution (selectivity to products) are provided at the half lifetime and calculated on the basis of carbon atoms; C_{1-5}^0 represents alkanes with 1–5 carbon atoms, whereas $C_2^=$–$C_5^=$ represent ethene to pentenes.

[c] P/E is the selectivity ratio of propene to ethene.

[d] C_4-HTI represents the hydrogen transfer index, which is calculated from the selectivity to butane (C_4^0) and butene ($C_4^=$) by $n(C_4^0)/(n(C_4^0) + n(C_4^=))$ in the products.

[e] Catalytic lifetime is defined as the time on stream when the conversion of methanol drops to 90%.

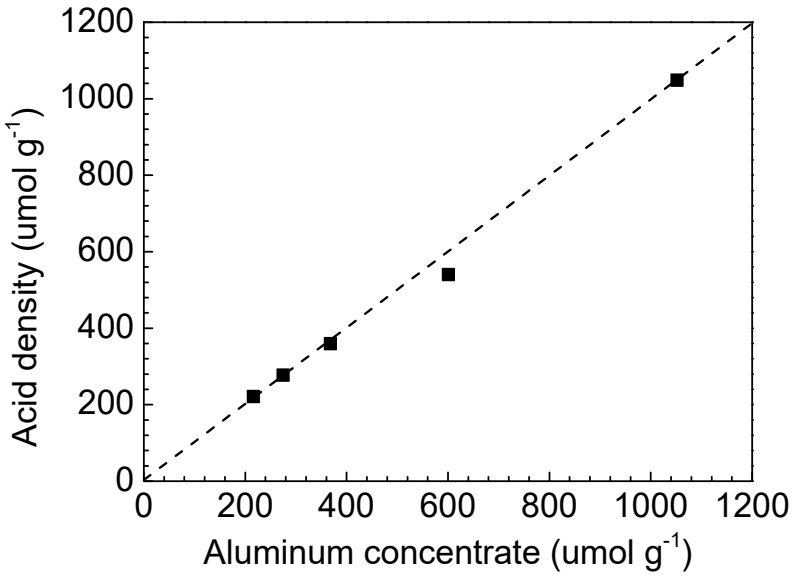

Figure S1. The linear relationship between aluminum concentration determination by ICP-AES and total acid density measured by NH_3-TPD experiments in H-M22-*x* zeolites.

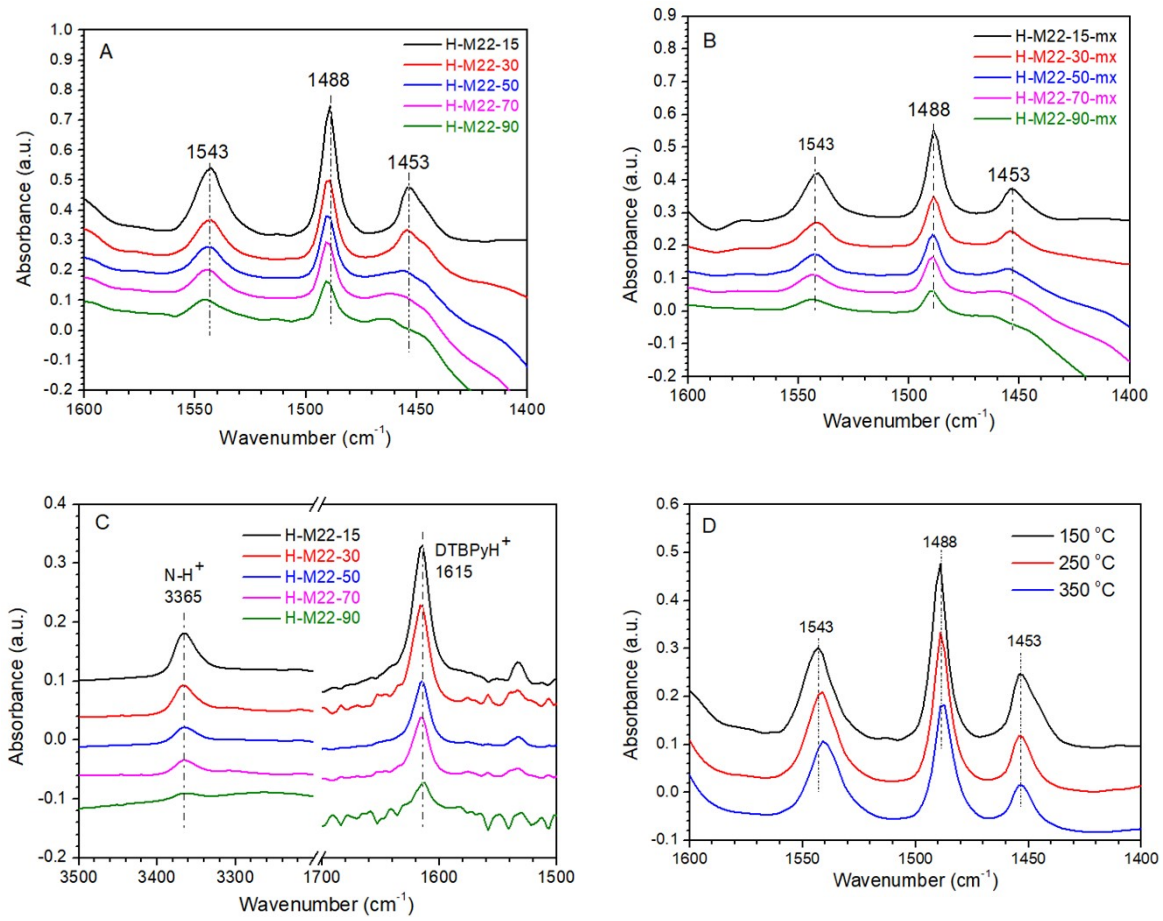

Figure S2 Determination of acid distribution and acid strength by FT-IR spectra of pyridine adsorption (Py-IR) and 2,6-di-tert-butylpyridine adsorption (DTBPy-IR). The Py-IR spectra determined at 150 °C of (A) H-M22-x zeolites; (B) H-M22-x-mx zeolites; (C) the DTBPy-IR spectra determined at 150 °C of H-M22-x zeolites; (D) the Py-IR spectra of H-M22-15 zeolite determined at 150, 250 and 350 °C.

The Pyridine adsorption bands in Py-IR spectra at 1543 cm^{-1} and 1453 cm^{-1} are attributed to pyridinium ions (PyH^+) formed by pyridine adsorbed on Brönsted acid sites, and to pyridine coordinated to Lewis acid sites (PyL), respectively. The bands at 1488 cm^{-1} are contributed by both PyH^+ and PyL. The bands at 1543 cm^{-1} and 1453 cm^{-1} are used to estimate the densities of Brϕnsted acid sites (BAS) and Lewis acid sites (LAS), respectively, according to Madeira et al[1].

The total Brϕnsted acid sites (B_{total}) and total Lewis acid sites (L_{total}) in H-M22-x zeolites are

[1] F. Ferreira Madeira, K. Ben Tayeb, L. Pinard, H. Vezin, S. Maury and N. Cadran, *Appl. Catal. A: General*, 2012, **443–444**, 171–180.

calculated based on the Py-IR spectra determined at 150 °C of H-M22-x zeolites (Figure S2 A). The Py-IR spectra determined at 150 °C of H-M22-x-mx zeolites (Figure S2 B) are used to calculate the residual Brϕnsted acid sites after selectively poisoning the supercages in zeolite. Thus, the Brϕnsted acid sites in the supercages (B_{sup}) of H-M22-x zeolites can be estimated by the differences the quantitative results of Figure S2 A and Figure S2 B.

As shown in Figure S2 C, the adsorption bands at 3365 cm^{-1} and 1615 cm^{-1} in DTBPy-IR spectra of H-M22-x zeolites can be attributed to N-H stretching vibration and ring vibration mode in $DTBPyH^+$, which are characteristic of 2,6-di-tert-butylpyridine adsorption on Bronsted acid sites[2]. The Brϕnsted acid sites in the external pocket of H-M22-x zeolites (B_{poc}) are estimated from the adsorption band at 1615 cm^{-1} of the DTBPy-IR spectra determined at 150 °C, according to the Corma[3], Góra-Marek[4] and co-workers. Therefore, the density of BAS in the sinusoidal channels of H-M22-x zeolites can be calculated by the equation: $B_{sin} = B_{total}-B_{sup}-B_{poc}$.

The acid strength of H-M22-x zeolites are calculated based on the Py-IR spectra determined at different desorption temperatures; for example, the Py-IR spectra of H-M22-15 determined at 150, 250 and 350 °C are given in Figure S2D. The strong BAS and LAS were calculated from the Py-IR spectra recorded at 350 °C. The medium BAS and LAS were estimated from the difference of Py-IR spectra recorded at 350 °C and that of 250 °C. The weak BAS and LAS were estimated from the difference of Py-IR spectra recorded at 250 °C and that of 150 °C.

[2] K. Góra-Marek, K. Tarach and M. Choi, J. Phys. Chem. C, 2014, 118, 12266–12274.

[3] A. Corma, U. Diaz, V. Fornés, J. M. Guil, J. Martínez-Triguero and E. J. Creyghton, J. Catal., 2000, 191, 218–224.

[4] K. Góra-Marek, K. Tarach and M. Choi, J. Phys. Chem. C, 2014, 118, 12266–12274.

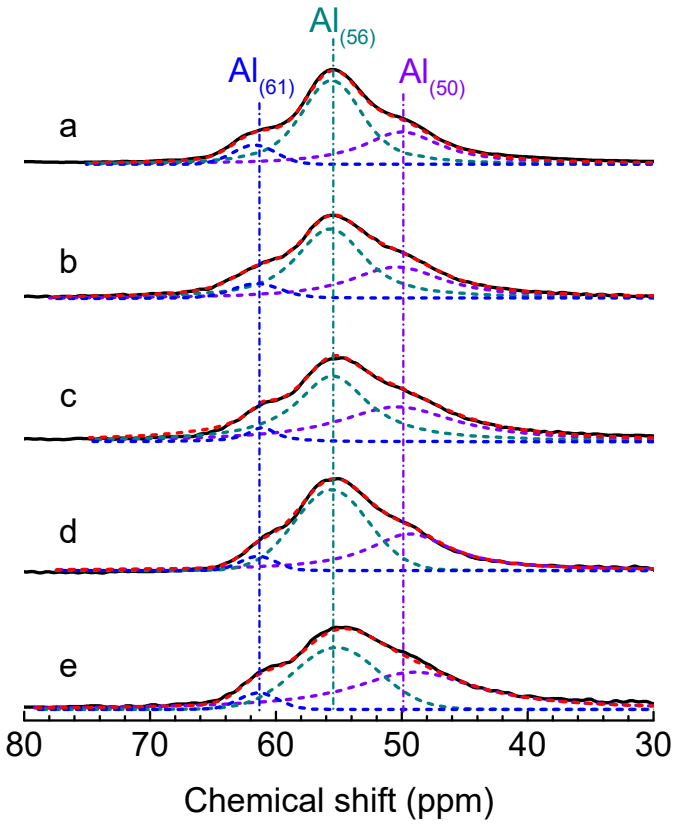

Figure S3. Deconvolution of the ^{27}Al MAS NMR spectra (the number of scans used was 10000) of the H-MCM-22 zeolites with different Si/Al ratios: (a) H-M22-15; (b) H-M22-30; (c) H-M22-50; (d) H-M22-70 and (e) H-M22-90. The black lines are experimental spectra.

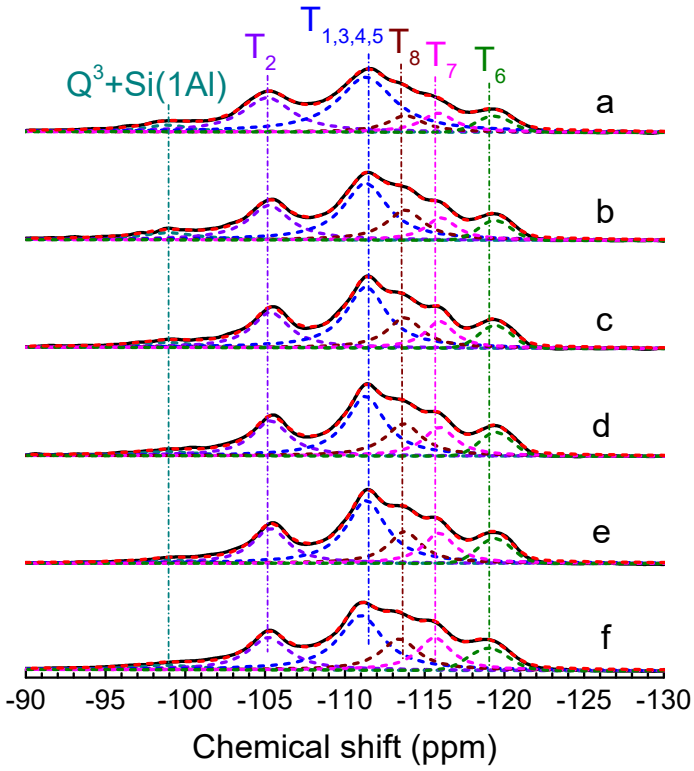

Figure S4. Deconvolution of the ^{29}Si MAS NMR spectra (the number of scans used was 960) the H-MCM-22 zeolites with different Si/Al ratios: (a) H-M22-15; (b) H-M22-30; (c) H-M22-50; (d) H-M22-70 and (e) H-M22-90, and aluminum-free borosilicate (f) H-B-MWW. The black lines are experimental spectra.

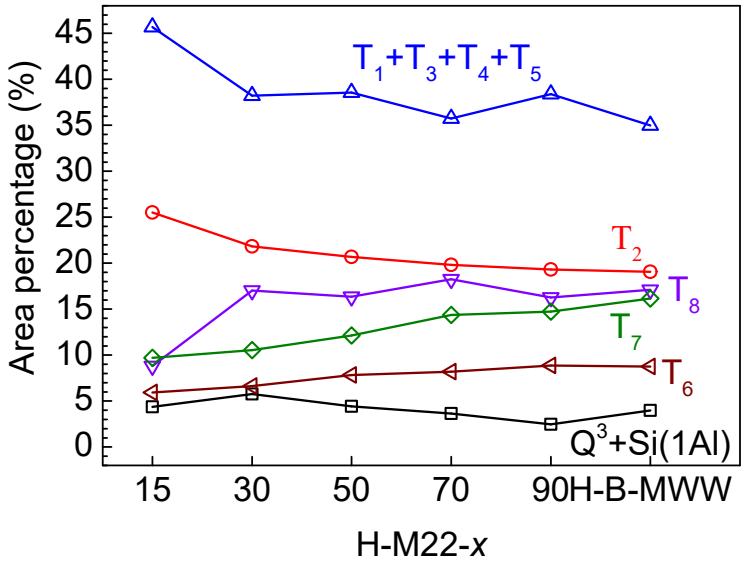

Figure S5. Area percentages of the fitted peaks obtained from the deconvolution of the ^{29}Si MAS NMR spectra of the H-M22-*x* zeolites.

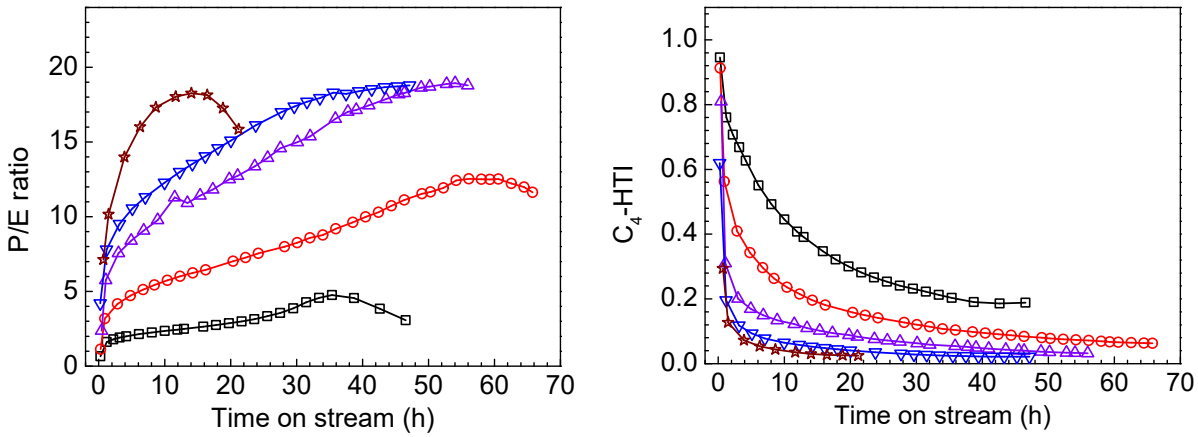

Figure S6. P/E ratio and C_4-HTI value as a function of time on stream in MTH over (□) H-M22-15; (○) H-M22-30; (△) H-M22-50; (▽) H-M22-70 and (☆) H-M22-90 at 450 °C with a methanol WHSV of 2 h^{-1}. P/E ratio is the selectivity ratio of propene to ethene, whereas C_4-HTI value represents the hydrogen transfer index calculated from the selectivity of butane (C_4^0) and butene ($C_4^=$) by $n(C_4^0)/(n(C_4^0) + n(C_4^=))$ in the products.

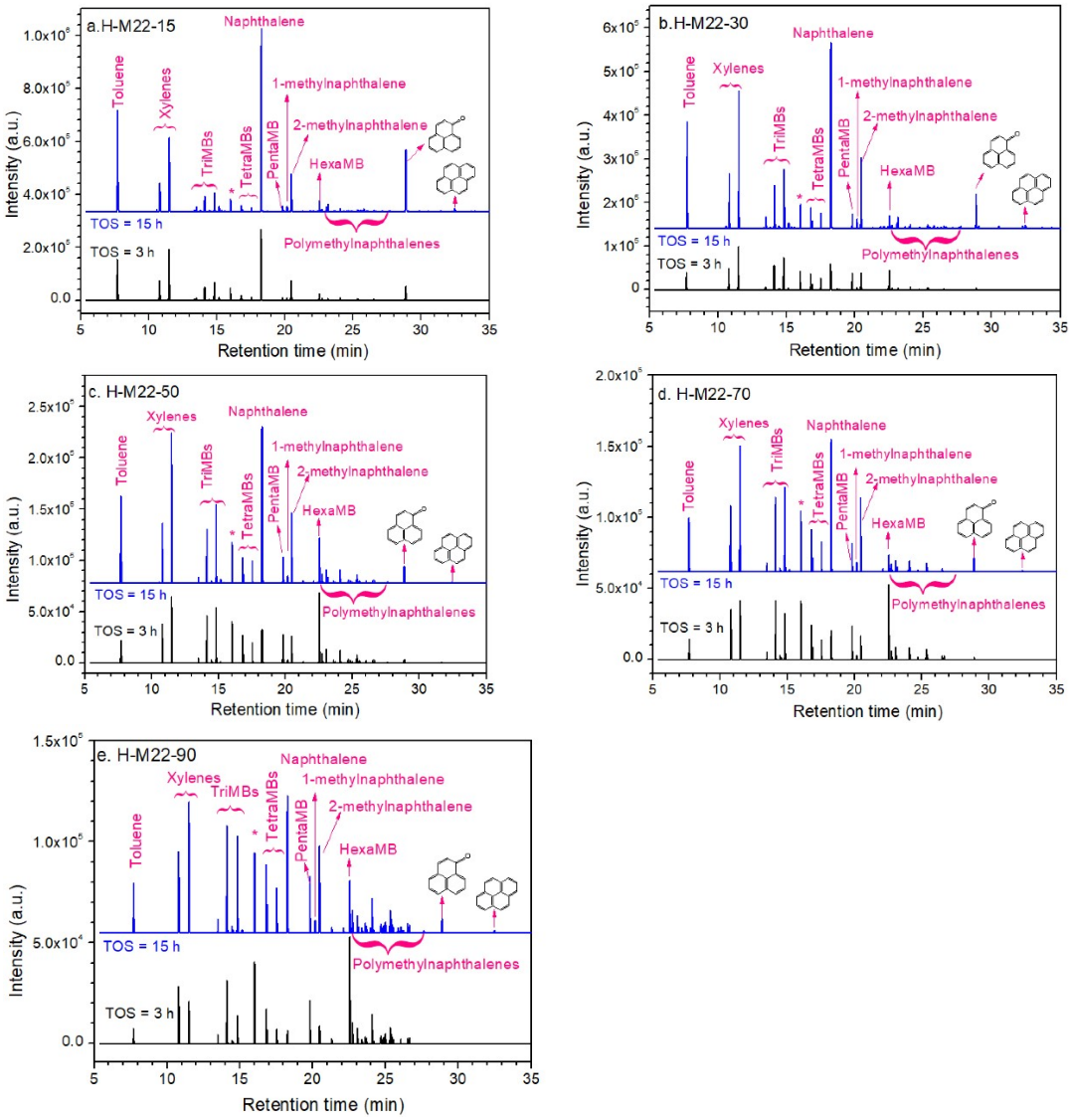

Figure S7. GC-MS total ion chromatograms of carbonaceous species retained in H-M22-x zeolites at the time on stream (TOS) of 3 h and 15 h for MTH at 450 °C with a methanol WHSV of 2 h^{-1} over (a) H-M22-15; (b) H-M22-30; (c) H-M22-50; (d) H-M22-70 and (e) H-M22-90. The asterisk (*) represents the internal standard (I.S., hexachloroethane)，and each spectra are normalized to I.S. intensity; triMB, tetraMB, pentaMB and hexaMB represent trimethylbenzene, tetramethylbenzene, pentamethylbenzene and hexamethylbenzene, respectively.

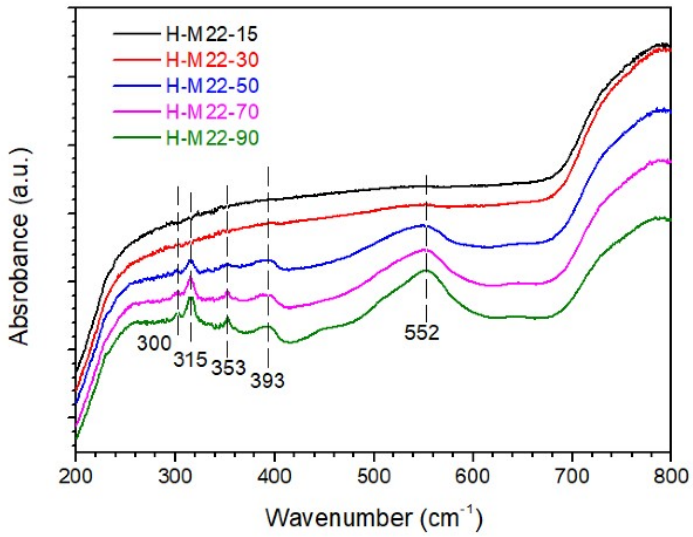

Figure S8. UV-vis spectra of completely deactivated (a) H-M22-15; (b) H-M22-30; (c) H-M22-50; (d) H-M22-70 and (e) H-M22-90 zeolites after MTH reactions (as shown in Figure 8).